THE ENVELOPE OF REACHABLE ASTEROIDS OF M-ARGO INTERPLANETARY CUBESAT

F. Topputo[(1)], C. Giordano[(1)], V. Franzese[(1)], Y. Wang[(1)], E. Cruz[(2)], F. Perez-Lissi[(3)], R. Walker[(3)]

[(1)]Department of Aerospace Science and Technology, Politecnico di Milano, Via la Masa 34, 20156 Milano, Italy
[(2)]GomSpace Luxembourg, 11 Boulevard du Jazz, L-4370 Belval, Luxembourg
[(3)]European Space Research & Technology Centre (ESTEC), ESA, Postbus 299, 2200 AG, Noordwijk, The Netherlands

ABSTRACT

The Miniaturised Asteroid Remote Geophysical Observer (M-ARGO) is planned to be the first standalone deep-space CubeSat mission to rendezvous with and characterise a near- Earth asteroid. M-ARGO is a 12U CubeSat equipped with a miniaturised electric propulsion system. To this aim, it is essential to assess the attainable set of target asteroids. We show the original procedure developed to assess the reachable NEO targets and the subsequent down-selection process. Our analyses show that approximately 150 minor bodies are found potentially reachable when departing from Sun-Earth L2 within a 3-year transfer duration. Out of these, 41 targets have been down-selected, and a short list of the 5 most promising objects has been extracted. Overall, M-ARGO has the potential to enable a completely new class of low-cost, deep space exploration missions.

1 INTRODUCTION

ESA has funded several interplanetary CubeSat mission studies like M-ARGO (Miniaturized Asteroid Remote Geophysical Observer) [1], LUMIO (Lunar Meteoroid Impacts Observer) [2], and CubeSats along the Hera mission [3,4]; NASA has funded several SmallSat deep-space mission studies after Mars Cube One (MarCO) [5]. M-ARGO is planned to be the first ESA stand-alone CubeSat mission to rendezvous with a near-Earth asteroid (NEA) [6]. The M-ARGO concept was initially developed by ESA's Concurrent Design Facility (CDF) team in 2017 [7]. The Phase A study was performed in 2019-2020 with GomSpace Luxembourg and Polimi to assess mission feasibility including NEO target selection, mission analysis, spacecraft design, and programmatic plan.

The M-ARGO mission objectives are: (1) To demonstrate the capability of CubeSat nano-spacecraft systems to independently explore deep space for the first time; (2) To rendezvous with a Near-Earth Object (NEO) and characterize its physical properties for the presence of in-situ resources; (3) To advance miniaturized technologies currently under development in Europe; (4) To test autonomous GNC techniques and components performance during transfer to target object.

This work deals with the NEO targets screening for the M-ARGO mission. The list of asteroids has been retrieved by the Minor Planet Center and filtered considering time-optimal and fuel-optimal transfers from the Sun-Earth L2 point to the asteroids location. Then, a short-list of 5 candidate targets is produced by a working group made by ESA, GomSpace, Politecnico di Milano and the Small Body community. These targets have been later found reachable by a dedicated mission analysis, where mission-dependent constraints have been enforced.

2 APPROACH

The objective of the M-ARGO mission is to rendezvous with a near-Earth asteroid to characterize its physical properties and assess the potential for future resource exploitation. Thus, it is required to identify the subset of asteroids that are reachable considering the constraints of a 12U deep-space CubeSat. Figure 1 shows the approach followed to filter the database of known asteroids to produce the reachable asteroids shortlist. Note that the final shortlist and the final target selection are made by a working group involving ESA, the small-body community, and the M-ARGO consortium (GomSpace Luxembourg and Politecnico di Milano). The procedure is detailed in the following.

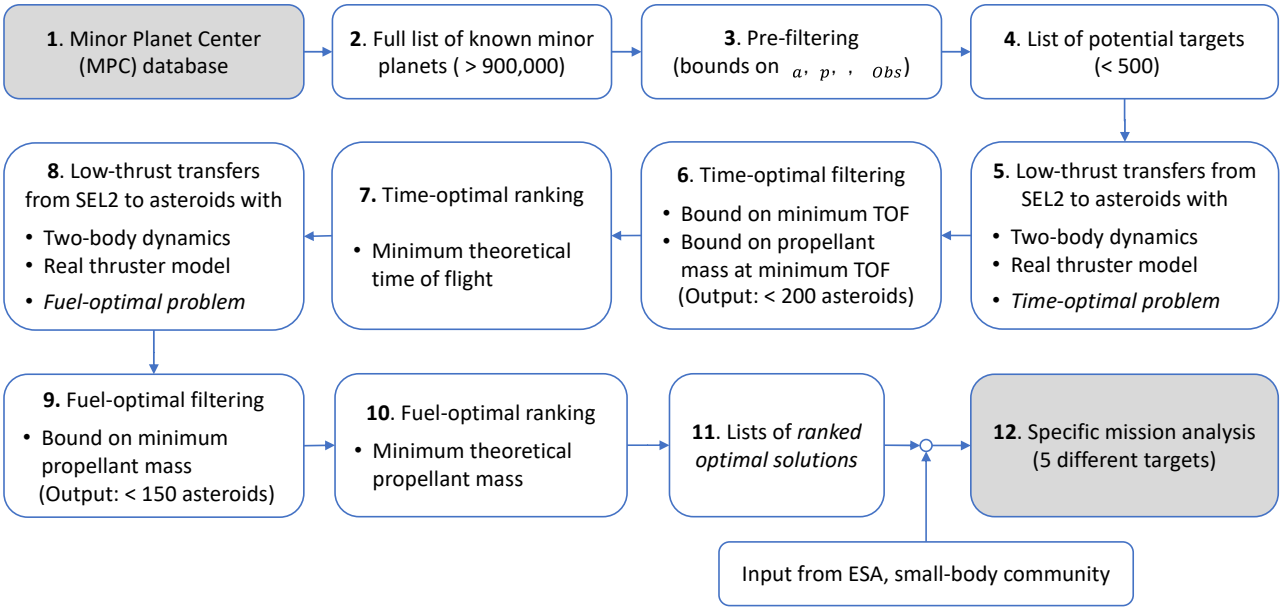

Figure 1: Methodology of the NEO target screening.

1-2 Database retrieval. The Minor Planet Center (MPC) Database is considered as the source of information for the minor planets in the Solar System. It comprehends the designation and the orbit computation of all the discovered minor planets and it is updated daily. More than 900,000 objects are accounted for as of October 2020.

3-4 Pre-Filtering. The full list of asteroids is prefiltered using ranges of orbital parameters. Educated guesses on these parameters have been inferred from [6]. These involve capping the aphelion, bottoming the perihelion, and bounding the inclination as well as the number of observations. This filtering reduces the full list of asteroids to a preliminary list of approximately 500 potential targets.

5-6 Time-optimal transfers. A massive search is conducted to compute time-optimal transfers to each of the asteroids in the preliminary list. The optimisation considers the two-body problem with a realistic thruster model, departure from Sun–Earth L2, and a three-year departure window. The aim of this step is to determine the minimum theoretical transfer time to each asteroid for each departure epoch. The objects whose minimum transfer time is greater than three years are filtered-out.

7 Time-optimal ranking. The filtered time-optimal solutions are ordered to produce a time-optimal ranking. The number of targets is then reduced to approximately 170 objects.

8-9 Fuel-optimal transfers. The objects resulting feasible after the time-optimal analysis are processed under the perspective of a fuel-optimal optimisation, using the same model and boundary conditions as in the time-optimal optimisation. This analysis finds the minimum propellant mass for each combination of departure epoch and transfer time. The objects whose minimum required propellant mass is greater than 2.8 kg are excluded from the list.

10 Fuel-optimal ranking. The fuel-optimal solutions as output of step 9 are ordered to produce a fuel-optimal ranking made of approximately 150 reachable objects.

11 Lists of ranked optimal solutions. The ranked lists of time-optimal and fuel-optimal solutions produced as output of the filtering chain has been examined by GomSpace, Politecnico di Milano, the small body community, and ESA. The 5 shortlisted targets have been the subject of a dedicated mission analysis (step 12).

3 MINOR PLANETS DATABASE FILTERING

The Minor Planet Center accounts for more than 900,000 objects in the Solar System. Figure 2a shows the semi- major axis (a) versus the eccentricity (e) for all the observed objects as a scatter plot (black dots), while Figure 2b displays the semi-major axis (a) versus the inclination (i) for the same bodies (black dots). The subset of potential targets has been defined by restricting the aphelium (r_a) upper bound (UB) to 1.25 AU and the perihelium (r_p) lower bound (LB) to 0.75 AU. Moreover, in order to comply with realistic CubeSat propulsive capabilities, an upper bound on the inclination equal to 10 deg has been set. Finally, a lower bound of 10 observations (N_{obs}) is enforced to assure accuracy in the orbital elements of the asteroids.

The constraints in terms of r_a, r_p, and i are shown in Figure 2. The solid and the dashed lines in Figure 2 (left) represent the projection of the perihelium and aphelium bounds on the (a, e) plane. The solid horizontal line in Figure 2 (right) is the upper bound on the inclination. The asteroids that satisfy the search space bounds are those corresponding to the black dots in Figure 2.

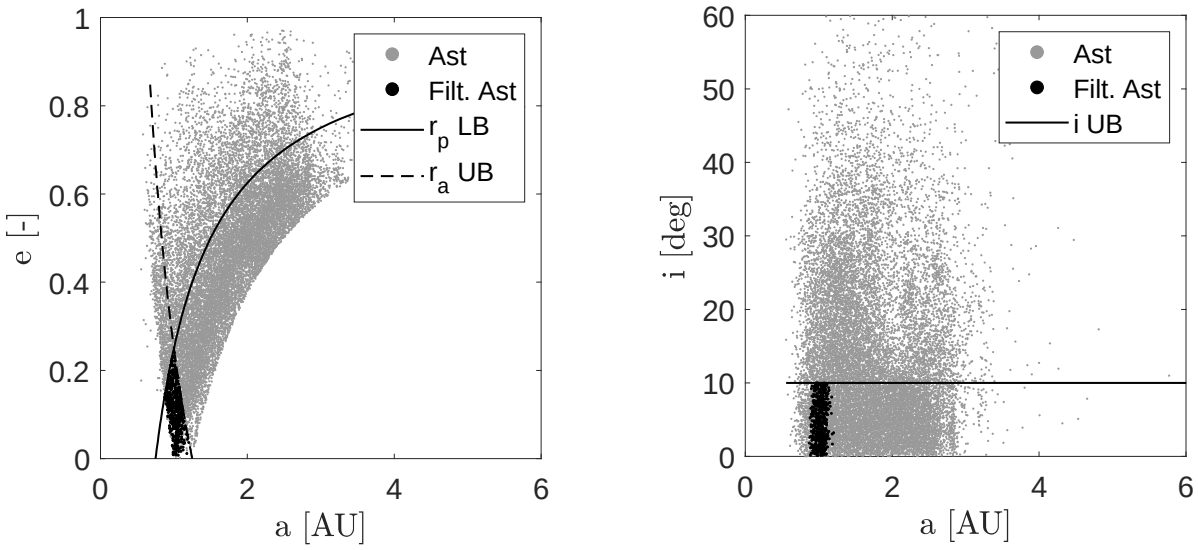

Figure 2: Minor planets semi-major axis (a), eccentricity (e), and inclination (i). Filtering bounds in solid and dashed lines; filtered asteroids highlighted in black.

Figure 3 shows the estimated size versus the rotational period of the asteroids catalogued in the Asteroid Lightcurve Database (LCDB). The plot highlights the "spin barrier" (dashed line). Most of the big asteroids (with a diameter larger than 1 km) lie below the spin barrier, meaning that they have a rotational period higher than 2 hours. The small asteroids have a rotational period that can be in the order of 1 hour or less. The filtered asteroids are in black dots in Figure 3; some of them lie in the region of the fast rotators.

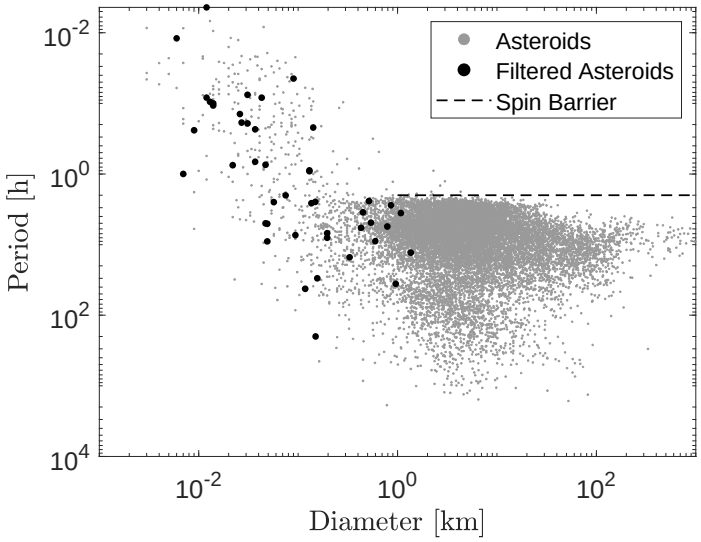

Figure 3: Rotational period vs diameter of minor planets. Filtered asteroids in black.

4 ASSUMPTIONS

This section reports the assumptions made for the mission and the spacecraft as inputs to the time-optimal and fuel-optimal filtering steps.

4.1 Mission and spacecraft data

The departure from the Sun–Earth L2 point (SEL2) is set in the window 1 Jan 2023—31 Dec 2024. The considered transfer duration is up to 3 years, and the close-proximity operations last up to 6 months. The spacecraft mass is 26.4 kg and the propellant mass is 2.8 kg. The Sun-projected area is 0.30 m^2 and the reflectivity coefficient is 1.3.

4.2 Thruster model

The trajectory design implements a realistic thruster model, that is, a model mapping maximum thrust and specific impulse variation over the instantaneous input power. The thruster model assumes that both the maximum thrust, T_{max}, and the specific impulse, I_{sp}, depend on the instantaneous engine input power, P_{in}, which in turn is a function of the Sun distance, r. These functions have been handled using fourth-order polynomials, which represent surrogate models of the miniaturized ion thruster as well as the power production and distribution units to be used in M-ARGO. The detailed thruster model can be found in [8,9], while its graphical representation is reported in Figure 4. By inspection of Figure 4 we notice that the thruster input power is bounded within a minimum and maximum value, $P_{in,min}$ and $P_{in,max}$, respectively, for technological limits.

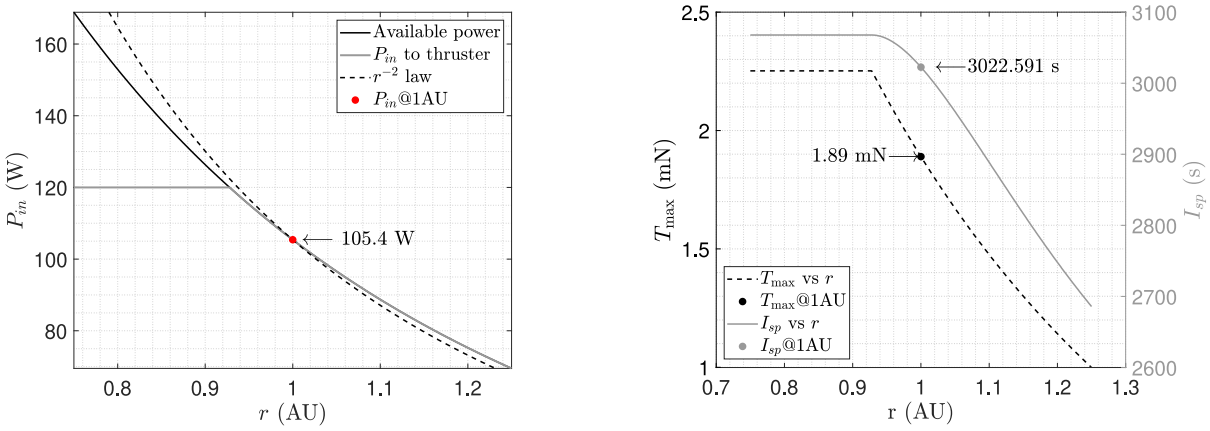

Figure 4: Graphical representation of the realistic thruster model.

5 TIME-OPTIMAL TRANSFERS

Performing a time-optimal search in a two-year departure window for different objects requires solving approximately 3.3×10^5 optimisation problems with a one-day time discretisation. The indirect solver LT2.0 (Low- Thrust Trajectory Optimiser 2.0) internally developed at Politecnico di Milano [10] has been adapted for this purpose. The dynamic model used is a standard two-body problem implementing the realistic thruster model in Section 4.2.

5.1 Methodology

An indirect approach is chosen to solve a myriad of optimal control problems in an efficient way. The essence is using the first-order necessary conditions to state a two-point boundary value problem (TPBVP) and the associated shooting function. A zero-finding problem is then employed to solve for the initial costate. The approach as well as the solution method are the ones given in [11].

The time-optimal transfers for the filtered asteroids in Section 4 are solved with the departure window in Section 4.1. The Sun-centered two-body problem is employed. Numerical experiments show that solutions continued in higher fidelity models, which consider the gravitational acceleration of the Sun and the planets, the solar radiation pressure, and the non-spherical gravity, feature negligible differences from those found in this model. An average increase of 5% in propellant mass is found, mainly to counteract the gravity of the Earth, when the spacecraft is close to L2 [9].

Consistently with the thruster model in Section 4.2, we have assumed that both the maximum thrust, T_{max}, and the specific impulse, I_{sp}, are assumed to vary with the engine input power P_{in}, which is in turn function of the Sun distance. The initial heliocentric position and velocity vectors, as well as the state of the target asteroids, are retrieved by their SPICE kernel. Optimising the transfer time produces solutions whose thrust is always set at the maximum available value. While these solutions are not feasible in practical applications, they yield the minimum theoretical transfer time, τ_{min}, which can be used to prune the search space of feasible solutions.

5.2 Search space pruning

For each of the asteroids processed, τ_{min} is retrieved, as well as its corresponding propellant mass $m_p(\tau_{min})$. The two quantities are reported in Figure 5 in the form of cumulative distribution functions. This information has been used to further narrow the set of asteroids that can be reached by M-ARGO. Indeed, considering that the real transfer time is longer than the one resulting from time-optimal computations, the following criteria have been used: 1) Minimum theoretical transfer time lower than 900 days (there are 299 asteroids out of the ones processed satisfying this condition; see Figure 5 left); 2) Minimum propellant mass lower than 4 (there are 181 asteroids out of the one processed whose minimum propellant mass is below this threshold; see Figure 5 right).

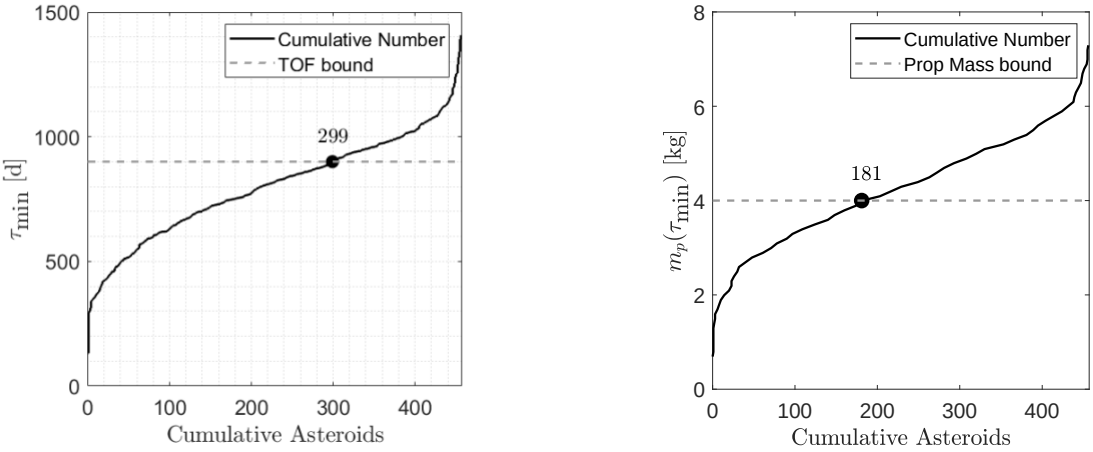

Figure 5: Cumulative number of asteroids for increasing τ_{min} and associated $m_p(\tau_{min})$. Filtering bounds in dashed lines; the number indicates the asteroids below the threshold.

We further impose that these two conditions have to be verified simultaneously. The graphical representation in Figure 6 shows that the propellant mass condition is the more stringent one. As a result of this pruning process, we have 172 asteroids ranked after the time-optimal screening. The ranking can be consulted in [9]; it is the input of the fuel-optimal exercise as per Figure 1.

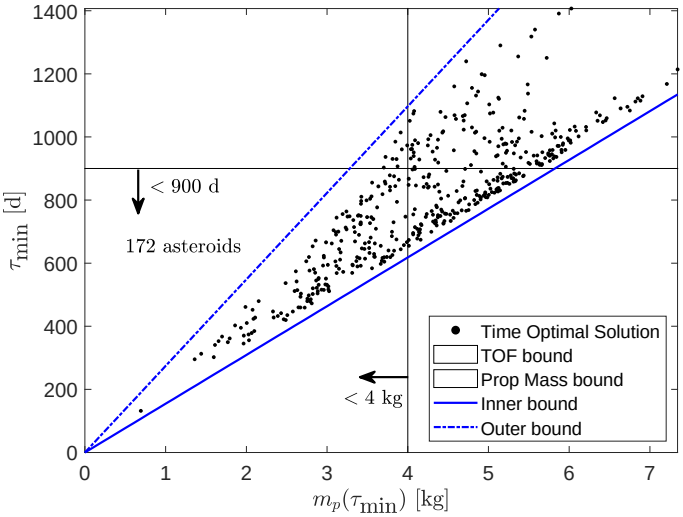

Figure 6: Time of flight for the time-optimal solutions against the associated propellant mass. filtering bounds in black solid lines; the number indicates the asteroids below both thresholds.

6 FUEL-OPTIMAL TRANSFERS

The 172 potential targets that passed the time-optimal pruning have been processed under the perspective of a fuel-optimal step. It is worth highlighting that the fuel-optimal process widens the variable space as both the departure epoch t_0 and the time of flight *tof* are let to vary. That is, while time-optimal problems have a one-dimensional search space (t_0), the fuel-optimal problems have a two-dimensional search space ([t_0 , *tof*]). A two-dimensional grid is therefore used for the porkchop plots.

6.1 Methodology

The minimum-fuel optimisation has been performed by using the same model as in the minimum-time optimisation. For each departure day t_0, the time of flight *tof* is bottomed by the corresponding minimum transfer time $\tau(t_0)$ and capped by the three-year upper bound condition. This variable range has been discretised using a nonuniform grid, to ease efficiency. The boundary conditions are the asteroid position and velocity at the arrival epoch, retrieved from SPICE. The objective function is the used propellant mass. The detailed methodology is in [9].

6.2 Search space pruning

For the 172 asteroid processed, the minimum propellant mass, $m_{p,min}$, is retrieved, as well as the corresponding value of t_0 and *tof*. The global minimum propellant mass $m_{p,min}$ is shown in the form of a cumulative distribution function in Figure 7. This information has been used to further reduce the search space by enforcing the "up to 2.8 kg" requirement. It can be seen that 148 asteroids result feasible when enforcing this requirement.

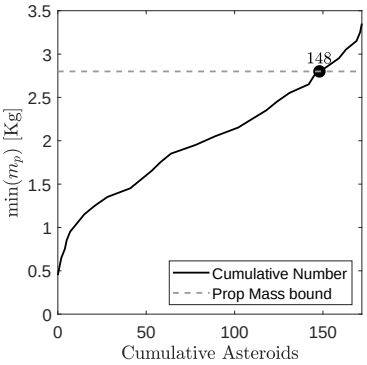

Figure 7: Cumulative number of asteroids for increasing global minimum propellant mass. Available propellant mass in dashed line; the number shows the number of asteroids below the threshold.

7 TARGETS SELECTION

With reference to the methodology developed for the NEO target screening, out of more than 900,000 minor bodies in the MPC database, 456 objects passed the pre-filtering, which was based on simple geometrical criteria. For these 456 objects, a minimum-time optimisation was carried out, and a subset made of 172 targets passed the pruning process when enforcing both a transfer time and a propellant mass thresholds (Section 5). These asteroids were processed under the perspective of a minimum-fuel optimisation, and a subset of them made of 148 reachable targets was found (Section 6).

The whole process undertaken as well as the intermediate results are summarised in [9]. The focus is on extracting a shortlist of 5 baseline asteroids out of the 148 reachable targets. This has been done through: 1) Statistical analysis of the reachable targets and their transfers; 2) Detailed analysis of pork chop plots; 3) Close-up analysis of the downselected targets. The analysis in 1)–2) produces the list of downselected asteroids (step #5 in Table 1), while the outcome of 3) is the list of the 5 targets selected (step #6 in Table 1).

Step	Target screening step	No. of objects
#1	Asteroids in the Minor Planet Center database	900,000+
#2	Potential targets after orbital parameters pre-filtering	456
#3	Possible targets after minimum-time optimisation and pruning	172
#4	Reachable targets after minimum-fuel optimisation and pruning	148
#5	Downselected targets after statistical, pork chop analysis	41

Table 1: NEO target screening process and results.

8 SHORTLIST OF TARGETS

Once the list of the 41 downselected targets has been defined, a deliberate choice has been made. This choice considers the available of information on the asteroid light-curve, spin-rate, and observability in the future to further downselect the targets.
As a result of this exercise, the three top picks for the initial selection are:

1. **2014 YD**: Known high spin rate close to spin bar- rier and favourable mission opportunity;
2. **2010 UE51**: #1 on time-optimal and fuel-optimal solution list;
3. **2011 MD**: Present in light curve database; Favourable mission opportunity.

Moreover, two more asteroids have been liberally chosen based on their solar distances, Earth distances, size/magnitude, departure opportunity, etc.; the two additional targets are:

4. **2000 SG344**: Chance for observation, higher in- clination, good OCC;
5. **2012 UV136**: Known spin rate, largest target size/brightest.

9 CONCLUSIONS

This paper has reported the NEO targets screening for the M-ARGO mission. In order to select the mission targets, a series of asteroids filtering activities have been performed to identify a subset of asteroids that are reachable by the M-ARGO CubeSat. The downselection procedure started by consulting the Minor Planet Center database and ended up with a set of 5 shortlisted targets. First, bounds on orbital elements have reduced the list of asteroids to 456 objects. Out of these, 172 objects require less than 3 years for the time-optimal solution, and 148 require less than 2.8 kg for the fuel-optimal solution. Then, out of 148 objects completely reachable by the M-ARGO CubeSat, 5 asteroids have been selected as potential targets for the mission. This filtering step was required to assess the mission feasibility in terms of availability of targets given the M-ARGO 12U CubeSat spacecraft and mission characteristics.

10 ACKNOWLEDGMENT

This work has been conducted under ESA Contract No. 4000127373/19/NL/AF.

11 REFERENCES

[1] R. Walker, D. Binns, C. Bramanti, M. Casasco, P. Concari, D. Izzo, D. Feili, P. Fernandez, J. Fernandez, P. Hager, et al. Deep-space CubeSats: Thinking inside the box. Astronomy & Geophysics, 59(5):5–24, 2018. DOI: 10.1093/astrogeo/aty237

[2] A. Cervone, F. Topputo, S. Speretta, A. Menicucci, E. Turan, P. Di Lizia, M. Massari, V. Franzese, C. Giordano, G. Merisio, D. Labate, G. Pilato, E. Costa, E. Bertels, A. Thorvaldsen, A. Kukharenka, J. Vennekens, R. Walker, LUMIO: A CubeSat for observing and characterizing micro-meteoroid impacts on the lunar far side, Acta Astronautica, 2022, DOI: 10.1016/j.actaastro.2022.03.032

[3] F. Ferrari, V. Franzese, M. Pugliatti, C. Giordano, and F. Topputo, Preliminary mission profile of Hera's Milani CubeSat, Advances in Space Research, 67, 2010-2029, 2021, DOI: 10.1016/j.asr.2020.12.034

[4] O. Karatekin, H. Goldberg, C.-L. Prioroc, V. Villa, Juventas Team, Juventas: Exploration of a binary asteroid system with a CubeSat. Proceedings of the International Astronautical Congress, IAC, 2019

[5] A. Klesh and J. Krajewski. MarCO: Cubesats to Mars in 2016. In 29th Annual AIAA/USU Conference on Small Satellites, pages 1–7, Logan, UT, 2015

[6] A. Mereta and D. Izzo. Target selection for a small low-thrust mission to near-Earth asteroids. Astrodynamics, 2(3):249–263, 2018. DOI: 10.1007/s42064- 018-0024-y

[7] R. Walker, D. Binns, C. Bramanti, M. Casasco, P. Concari, D. Izzo, D. Feili, P. Fernandez, J. Fernandez, P. Hager, et al. M-ARGO: Assessment of standalone interplanetary CubeSat mission. CDF Study Report, 2017

[8] V. Franzese, C. Giordano, Y. Wang, F. Topputo, H. Goldberg, A. Gonzalez, and R. Walker, Target Selection for M-ARGO Interplanetary CubeSat, 71st International Astronautical Congress, 12-14 October 2020

[9] F. Topputo, Y. Wang, C. Giordano, V. Franzese, H. Goldberg, F. Perez-Lissi, and R. Walker, Envelop of reachable asteroids by M-ARGO CubeSat, Advances in Space Research, 67, 4193-4221, 2021, DOI: 10.1016/j.asr.2021.02.031

[10] F. Topputo, D. Dei Tos, K. Mani, S. Ceccherini, C. Giordano, V. Franzese, and Y. Wang. Trajectory design in high-fidelity models. In 7th Inter- national Conference on Astrodynamics Tools and Techniques (ICATT), 6-9 November 2018, Oberp- faffenhofen, Germany, 2018.

[11] C. Zhang, F. Topputo, F. Bernelli-Zazzera, and Y. Zhao. Low-thrust minimum-fuel optimization in the circular restricted three-body problem. Journal of Guidance, Control, and Dynamics, 38, 1501–1510, 2015, DOI: 10.2514/1.G001080